



1 **Non-negligible secondary contribution to brown carbon in autumn and winter:**
2 **inspiration from particulate nitrated and oxygenated aromatic compounds in**
3 **urban Beijing**

4

5

6 Yanqin Ren¹, Zhenhai Wu¹, Yuanyuan Ji¹, Fang Bi¹, Junling Li¹, Haijie Zhang¹, Hao
7 Zhang¹, Hong Li^{1*}, Gehui Wang^{2*}

8

9 ¹ State Key Laboratory of Environmental Criteria and Risk Assessment, Chinese
10 Research Academy of Environmental Sciences, Beijing 100012, China

11 ² Key Lab of Geographic Information Science of Ministry of Education of China,
12 School of Geographic Sciences, East China Normal University, Shanghai 200142,
13 China

14

15

16 *Corresponding authors: Dr. Gehui Wang/ Dr. Hong Li

17 E-mail address: ghwang@geo.ecnu.edu.cn / lihong@craes.org.cn



18 **Abstract**

19 Nitrate aromatic compounds (NACs) and oxygenated derivatives of polycyclic
20 aromatic hydrocarbons (OPAHs) play vital roles within brown carbon (BrC),
21 influencing both climate dynamics and human health to a certain degree. The
22 concentrations of these drug classes were analyzed in PM_{2.5} from an urban area in
23 Beijing during the autumn and winter of 2017–2018. There were four heavy haze
24 episodes during the campaign; two of which happened prior to heating whereas the
25 other two after heating. During the entire course of sampling, the mean total
26 concentrations of the nine NACs and the eight OPAHs were 1.2–263 and 2.1–234 ng m⁻³,
27 respectively. The concentrations of both NACs and OPAHs were approximately 2–3
28 times higher in the heating period than before heating. For NACs, the relative molecular
29 composition did not change significantly before and during heating, with 4-
30 nitrocatechol and 4-nitrophenol demonstrating the highest abundance. For OPAHs, 1-
31 Naphthaldehyde was the most abundant species before and during heating, while the
32 relative proportion of Anthraquinone increased by more than twice, from 13% before
33 heating to 31% during the heating. In Beijing's urban area during autumn and winter,
34 significant sources of NACs and OPAHs have been traced back to automobile emissions
35 and biomass-burning activities. Interestingly, it was observed that the contribution from
36 coal combustion increased notably with the onset of heating during this period. It is
37 worth noticing that the secondary generation of BrC was important throughout the
38 whole sampling period, which was manifested by the photochemical reaction before



39 heating and the aqueous reaction during heating. It was further found that the haze in
40 autumn and winter was nitrate-driven before heating and SOC-driven when heating
41 began, and the secondary formation of BrC increased significantly in pollution events,
42 particularly during heating.

43 **1 Introduction**

44 As an important light-absorbing material, brown carbon (BrC) has garnered
45 increasing attention in recent years (Jiang et al., 2023; Yi Chen et al., 2022; Song et al.,
46 2022; Cai et al., 2022; Zhang et al., 2021; Liu et al., 2023; Ren et al., 2023; Ren et al.,
47 2022). BrC could not only directly absorb solar energy, but also indirectly contribute to
48 climate change by promoting the evaporation of water and the dispersal of clouds
49 (Laskin et al., 2015; Huang et al., 2018). In addition to its significant climate effects,
50 BrC also has potential adverse effects on human health on account of its strong
51 mutagenic, cytotoxic, and carcinogenic properties (Teich et al., 2016).

52 Primary as well as secondary sources contribute to the atmospheric accumulation
53 of BrC (Zhu et al., 2021). Direct emissions of primary BrC come from burning biomass
54 and combustion of fossil fuels (Ni et al., 2021; Wang et al., 2020a; Lu et al., 2019a; Lu
55 et al., 2019b). Oxidation and aging processes in the atmosphere produce secondary BrC
56 (Wang et al., 2019; Wang et al., 2020c; Cheng et al., 2021; Jiang et al., 2023; Cai et al.,
57 2022). Toluene, phenol, benzene, and other aromatic hydrocarbons can be oxidized by
58 NO₃ or OH radical vapor phase in the presence of NO_x to produce nitrophenol or



59 nitrocatechol (Olariu et al., 2002; Sato et al., 2007; Iinuma et al., 2010; Ji et al., 2017).
60 VOCs emitted during biomass combustion and pyrolysis (such as cresol, catechol,
61 methyl catechol, etc.) can be oxidized to produce nitro-aromatic hydrocarbons (Iinuma
62 et al., 2010; Claeys et al., 2012; Finewax et al., 2018). Research on the source analysis
63 of brown carbon (BrC) frequently focuses on examining two key constituents: the
64 carbon component within humic-like substances (HULIS-C) and water-soluble organic
65 carbon (WSOC). These components are often studied to understand the origins and
66 properties of BrC in various environmental contexts. Secondary generation and burning
67 of biomass are the two main sources of HULIS in Guangzhou and Shanghai (Fan et al.,
68 2016; Zhao et al., 2016). In comparison with the water-insoluble BrC in the winter, the
69 contribution of non-fossil sources (for instance burning biomass) to water-soluble BrC
70 is 67% (Liu et al., 2018; Song et al., 2018). Coal combustion is presumably a significant
71 source of HULIS in the winter, in addition to burning biomass and secondary generation
72 (Tan et al., 2016). According to multiple studies conducted in Beijing, the primary
73 contributor to WSOC is secondary generation, accounting for 54% of its composition.
74 Following this, biomass burning contributes approximately 40%, while other primary
75 emission sources contribute a smaller proportion, making up only 6% (Du et al., 2014).
76 In Beijing, the percentages of biomass burning, coal combustion, and secondary
77 generation that contribute to atmospheric HULIS are 47%, 15%, and 39%, respectively.
78 The primary origins of HULIS show minimal association with motor vehicles and
79 industrial emissions (Li et al., 2019). According to Ma et al., secondary generation is
80 responsible for over 50% of HULIS in the non-heating season. Biomass burning



81 represents 21% of the HULIS content during this period. However, in the heating
82 season, approximately 40% of HULIS originates from biomass burning, while the
83 remaining 60% is contributed by diverse combustion sources like coal burning, waste
84 incineration, and vehicular emissions. Within this season, secondary generation
85 accounts for about 19% of the HULIS content (Ma et al., 2018).

86 The research suggests that various sources contribute to BrC, but their relative
87 impact varies depending on time and location. As a result, the chemical makeup, light
88 absorption characteristics, and concentrations of BrC show considerable variability.
89 This variability poses challenges in accurately assessing and forecasting the influence
90 of these sources on radiation and climate changes (Wang et al., 2020b; Yan et al., 2018;
91 Laskin et al., 2015). However, until recently, there was only a limited volume of
92 research pertaining to the sources and pathways of BrC leading to their generation in
93 the densely populated city environment. NACs and OPAHs are the primary focus of
94 this study because several studies have noted that nitrogen-containing aromatics,
95 polycyclic aromatic hydrocarbons (PAHs), and their derivatives are significant BrC
96 chromophores (Huang et al., 2018; Cai et al., 2022; Yi Chen et al., 2022; Wu et al.,
97 2020; Liu et al., 2023; Wang et al., 2020b). It is well-established that residential heating
98 plays a significant role in the substantial increase of anthropogenic pollutant emissions
99 during the winter season. From autumn to winter, there is a substantial rise in the
100 emission of aromatics-derived secondary organic aerosol (Ding et al., 2017), and
101 particle BrC is often detected especially in haze periods during the autumn and winter
102 (Liu et al., 2023). This study was conducted in the autumn and winter of 2017-2018 in



103 Beijing. Nine NACs and eight OPAHs were measured in PM_{2.5} samples, with a focus
104 on examining their sources, compositions, and concentration variations under various
105 air conditions. Specifically, emphasis was placed on investigating the contribution of
106 secondary generation to these two typical BrC species, particularly their involvement
107 in particle pollution processes during autumn and winter.

108 **2 Materials and Methods**

109 **2.1 Field observations**

110 PM_{2.5} was sampled at a height of 10m on the rooftop of a building at the Chinese
111 Research Academy of Environmental Sciences (CRAES), Beijing, China (40°02'N,
112 116°24'E). Using a high-volume sampler (1.13 m³ min⁻¹, Thermofisher Co., USA),
113 PM_{2.5} specimens were collected in the autumn and winter of 2017/2018. The sampling
114 process was executed from 8:00 to 19:30 during the day and from 20:00 to 7:30 in the
115 subsequent morning. The specimens and blanks were gathered using a pre-combusted
116 quartz fiber filter (at 450 °C for 6 h). A total of 4 field blanks and 122 PM_{2.5} samples
117 were acquired. Individual filters were sealed in a bag made from an aluminum foil bag
118 before sampling and analysis and placed in a freezer set at a temperature of -20 °C.

119 Using automatic equipment (CRAES Supersite for Comprehensive Urban Air
120 Observation and Research), meteorological parameters such as air temperature (T, °C)
121 and relative humidity (RH, %) along with gaseous pollutants (SO₂, NO₂, O₃, and CO)
122 were observed and measured at the same time.



123 **2.2 Chemical analysis**

124 The present study employed a pre-treatment comprising ultrasonic extraction and
125 derivatization in an attempt to analyze the organic species in the specimens. The details
126 of specimen extraction and derivatization have already been published (Wang et al.,
127 2009; Ren et al., 2021; Ren et al., 2023). In brief, filter aliquots were sectioned and
128 extracted with a methanol and dichloromethane (1:2 v/v,) mixture. Following the
129 concentration of the extracts to dryness, derivatization was carried out using a mixture
130 of N, O-bis-(trimethylsilyl) trifluoroacetamide [BSTFA+TMCS, (99:1), v/v] and
131 pyridine (5:1, v/v). Lastly, the derivatized samples were examined using gas
132 chromatography coupled with a mass spectroscopy detector (GC/MS: HP 7890A, HP
133 5975C, Agilent Co., USA). The extraction and derivatization methods described above
134 allowed for the simultaneous measurement of the samples' polar and non-polar
135 constituents.

136 Given that OPAHs and NACs were the main points of focus, this study
137 investigated a total of eight OPAHs and nine NACs. The nine NACs included 2,4-
138 dinitrophenol (2, 4-DNP), 4-nitrophenol (4NP), 3-methyl-4-nitrophenol (3M4NP), 4-
139 nitrocatechol (4NC), 4-methyl-5-nitrocatechol (4M5NC), 4-nitroguaiacol (4NGA), 5-
140 nitroguaiacol (5NGA), 3-nitro-salicylic acid (3NSA), and 5-nitro-salicylic acid (5NSA),
141 while the eight OPAHs encompassed 9-fluorenone (9-FO), benzanthrone (BZA), 1-
142 Naphthaldehyde (1-NapA), anthraquinone (ATQ), 1,4-chrysenequione (1,4-CQ),
143 benzo(a)anthracene-7,12-dione (7,12-BaAQ), 5,12-naphthacenequione (5,12-NAQ)
144 and 6H-benzo(cd)pyrene-6-one (BPYRone).



145 The elemental carbon (EC) and organic carbon (OC) content of individual PM_{2.5}
146 filter samples were analyzed using an Atmoslytic Inc. DRI model 2001 Carbon
147 Analyzer. This analysis followed the Interagency Monitoring of Protected Visual
148 Environments (IMPROVE) thermal/optical reflectance (TOR) protocol, involving the
149 examination of a 0.526 cm² punch from each specimen. The specifics of the above-
150 described techniques have been documented in literature (Li et al., 2016; Ren et al.,
151 2021).

152 **2.3 Evaluation of secondary BrC**

153 In this study, the contributions of secondary oxidation to the detected NACs and
154 OPAHs were evaluated by using a CO-tracer method, which is comparable to the EC-
155 tracer used for secondary OC quantification. Various methodologies have been
156 similarly adopted successfully in other studies (Liu et al., 2023; Cai et al., 2022).
157 Equation 1 and Equation 2 were respectively used to evaluate the secondary formation
158 of NACs and OPAHs.

$$159 \quad [\text{NACs}]_s = [\text{NACs}]_t - ([\text{NACs}]_t / [\text{CO}])_{\text{pri}} \times [\text{CO}] \quad (1)$$

$$160 \quad [\text{OPAHs}]_s = [\text{OPAHs}]_t - ([\text{OPAHs}]_t / [\text{CO}])_{\text{pri}} \times [\text{CO}] \quad (2)$$

161 [NACs]_s and [NACs]_t in Equation 1 refer to the NACs concentration produced by
162 secondary oxidation and the total amount of NACs, respectively. ([NACs]_t / [CO])_{pri}
163 represents the primary emission ratio of NACs in relation to combustion. This
164 calculation assumes that the primary source was predominant during the period, with
165 minimal secondary production. The ([NACs]_t / [CO])_{pri} was calculated in this work by
166 fitting the 15% lowest [NACs]_t / [CO] ratios observed during the entire sampling



167 duration. In equation 2 the concentration of OPAHs produced by secondary oxidation
168 and the total observed OPAHs are denoted by $[\text{OPAHs}]_s$ and $[\text{OPAHs}]_t$ respectively.
169 The concentration of CO is denoted by $[\text{CO}]$, while the primary emission ratio of
170 OPAHs in relation to combustion is represented by $([\text{OPAHs}] / [\text{CO}])_{\text{pri}}$, which was
171 calculated by fitting the lowest 15% $[\text{OPAHs}]_t / [\text{CO}]$ ratios observed in the entire
172 sample interval.

173 **3 Results and discussion**

174 **3.1 Variations in major components of $\text{PM}_{2.5}$ with respect to meteorological** 175 **conditions and gaseous pollution**

176 Based on the Beijing heating time, the entire period of the study was divided into
177 two phases: before heating (18 October to 14 November 2017) and during heating (15
178 to 23 November 2017; 23 December 2017 to 17 January 2018). Table 1 and Fig. 1
179 present the temporal fluctuations in meteorological factors, gaseous pollutant
180 concentrations, and the main $\text{PM}_{2.5}$ components in the two phases. The temperature (T)
181 and relative humidity (RH) were higher before heating (11 ± 3.8 °C and $49 \pm 26\%$) than
182 during heating (1.9 ± 4.4 °C and $23 \pm 15\%$), with average values amounting to $5.9 \pm$
183 5.9 °C and $35 \pm 25\%$, respectively. SO_2 concentrations during heating (4.3 ± 1.5 ppb)
184 were more than twice that before heating (2.1 ± 0.8 ppb), presumably because of the
185 increase in household coal burning for heating. The levels of NO_2 and NO remained
186 consistent before and during heating, suggesting that these pollutants were minimally



187 impacted by heating and were primarily influenced by mobile sources in Beijing. This
188 pattern seems to remain stable in the short term.

189 Fig.2 shows the variation in the chemical makeup of PM_{2.5} in the entire sampling
190 period, before and during heating, respectively. Secondary inorganic aerosols (SIA, i.e.
191 SO₄²⁻, NH₄⁺, and NO₃⁻) were identified as the leading constituents of PM_{2.5}, followed
192 by OM (1.6 times OC), with an average of 31.5% and 20.4% in the whole sampling,
193 respectively (Fig. 2a). Even though the PM_{2.5} concentrations remained relatively stable
194 during this period (as indicated in Table 1 and Fig. 2), there were significant changes
195 observed in the concentrations of SIA and OM, as well as their relative contributions to
196 PM_{2.5}. Before heating, SIA accounted for 41.9% of PM_{2.5}, which notably decreased to
197 23.1% during heating. This decline was primarily evident in the reduction of NO₃⁻.
198 Specifically, SO₄²⁻, NO₃⁻, and NH₄⁺ were measured at 5.5, 16, and 5.4 μg m⁻³,
199 respectively, according to Table 1. These values constituted 8.7%, 24.7%, and 8.5% of
200 PM_{2.5} before heating, as shown in Fig. 2b. Their concentrations decreased to 4.3, 6.8,
201 and 4.2 μg m⁻³ (Table 1). The relative contributions of NO₃⁻ to PM_{2.5} dropped
202 dramatically to 10.3% during heating, amounting to a drop of nearly 60%. Both SO₄²⁻
203 and NH₄⁺ experienced a roughly 25% decrease in their relative contributions to PM_{2.5},
204 as illustrated in Fig. 2c. The relative abundance of OM to PM_{2.5} increased from 18.6%
205 before heating to 21.9% during heating, with the average mass concentration of OC
206 showing an increase from 7.4 to 9.1 μg m⁻³ in the corresponding duration. The OC/EC
207 ratio also increased by 63% from 2.7 ± 3.3 before heating to 4.4 ± 3.7 during heating.
208 These significant changes in SIA and OM, including concentrations and the relative



209 contributions to PM_{2.5}, showed that primary organic aerosols and/or VOCs emissions
 210 were the leading contributors during the heating seasons due to household heating (Tan
 211 et al., 2018). The rise in mass concentrations of K⁺ and Cl⁻ indicated additional burning
 212 activities occurring during heating, aside from coal combustion, such as biomass
 213 burning (Bai et al., 2023; Li et al., 2022).

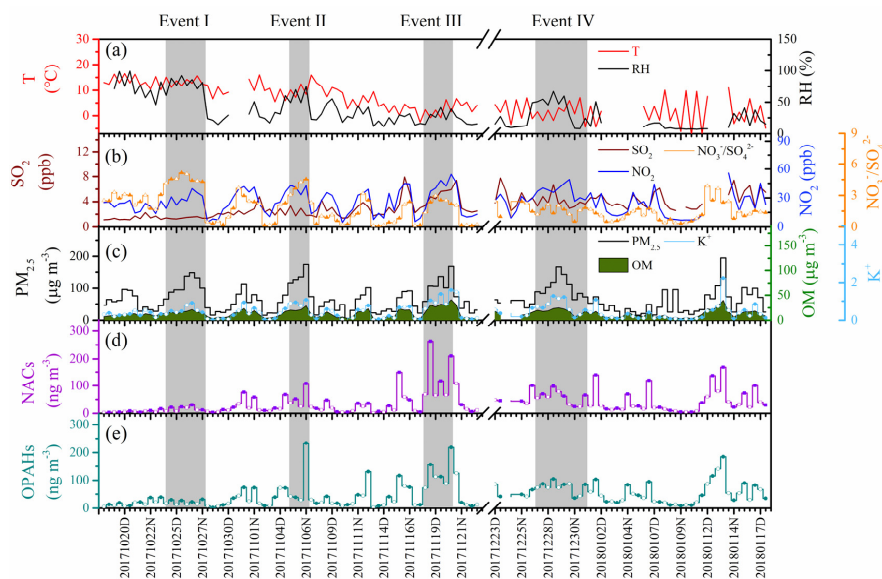
214

Table 1. Gaseous pollution concentrations and meteorological parameters and chemical constituents of PM_{2.5} during the sampling periods in Beijing.

	The whole sampling N=122	Before heating period 18/10–14/11, 2017 N=56	During heating period 15/11–23/11, 2017 23/12, 2017–17/1, 2018 N=66
Meteorological parameters			
Temperature, °C	5.9 ± 5.9 ((-7.5) – 16)	11 ± 3.8 (1.2 – 16)	1.9 ± 4.4 ((-7.5) – 11)
Relative humidity, %	35 ± 25 (7.1 – 99)	49 ± 26 (11 – 99)	23 ± 15 (7.1 – 67)
Gaseous pollutants, ppb			
SO ₂	3.2 ± 1.6 (1.1 – 7.9)	2.1 ± 0.8 (1.1 – 4.8)	4.3 ± 1.5 (2.2 – 7.9)
NO ₂	26 ± 13 (4.6 – 56)	25 ± 11 (4.6 – 43)	26 ± 14 (5.5 – 56)
NO	26 ± 28 (2.4 – 136)	28 ± 30 (2.4 – 136)	25 ± 26 (2.7 – 116)
CO	0.64 ± 0.55 (0.03 – 2.7)	0.81 ± 0.42 (0.12 – 1.6)	0.50 ± 0.61 (0.03 – 2.7)
Major components of PM_{2.5}, µg m⁻³			
PM _{2.5}	65 ± 40 (6.1 – 195)	64 ± 39 (6.1 – 175)	66 ± 41 (8.6 – 195)
OC	8.3 ± 5.0 (0.99 – 26)	7.4 ± 3.9 (1.0 – 18)	9.1 ± 5.8 (1.8 – 26)
EC	4.7 ± 4.7 (0.11 – 25)	4.9 ± 3.8 (0.11 – 17)	4.5 ± 5.3 (0.18 – 25)
OC/EC	3.7 ± 3.6 (0.96 – 21)	2.7 ± 3.3 (0.96 – 21)	4.4 ± 3.7 (1.0 – 17)
SO ₄ ²⁻	4.8 ± 4.2 (0.85 – 25)	5.5 ± 3.5 (0.86 – 13)	4.3 ± 4.7 (0.85 – 25)
NO ₃ ⁻	11 ± 14 (0.09 – 58)	16 ± 16 (0.09 – 58)	6.8 ± 8.8 (0.29 – 37)
NH ₄ ⁺	4.7 ± 4.9 (0.02 – 20)	5.4 ± 5.4 (0.02 – 20)	4.2 ± 4.5 (0.19 – 20)
K ⁺	0.43 ± 0.39 (0.02 – 2.2)	0.38 ± 0.27 (0.03 – 1.1)	0.48 ± 0.46 (0.02 – 2.2)
Cl ⁻	1.5 ± 1.6 (0.06 – 9.2)	1.0 ± 0.98 (0.06 – 4.5)	1.9 ± 2.0 (0.13 – 9.2)

215

216



217

218

Time (YYYYMMDD; D: daytime, N: nighttime)

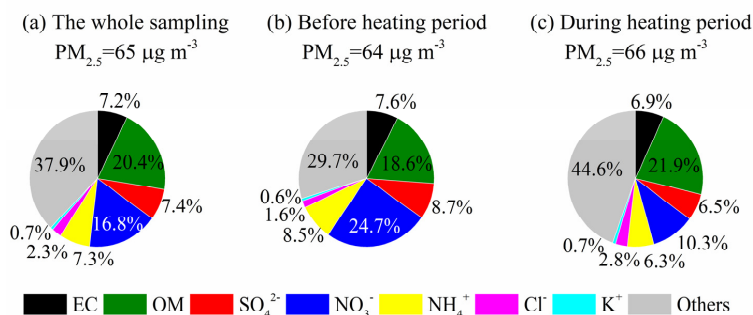
219

Fig.1 Time series of (a) RH and T, (b) SO₂ and NO₂, (c) PM_{2.5}, OM, and K⁺, (d) NACs and (e) OPAHs in the autumn and winter of urban Beijing. (Daytime is denoted by empty marks and the nighttime is represented by solid marks in the panel b–e. The pollution episodes, with elevated concentrations of daily PM_{2.5} more than 75µg m⁻³ in two successive days, have been marked in light gray).

222

223

224



225

226

Fig.2 Chemical constitution of PM_{2.5} in the entire sampling period (a), before (b), and during (c) heating periods, respectively.

227

228

3.2 Concentration and composition variations of BrC compounds

229

This work quantified nine NACs and eight OPAHs. The corresponding

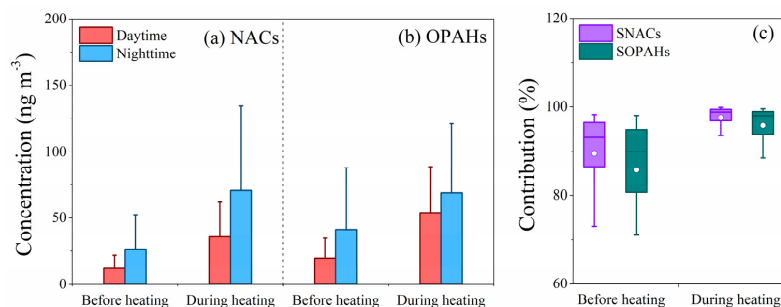


230 concentrations and compositions have been presented in Fig. 3 and Table S1
231 (supporting information).

232 As seen in Table S1, during the entire sampling, the total concentrations of NACs
233 ($\sum 9\text{NACs}$) and their corresponding contribution to OM ($\sum 9\text{NACs}/\text{OM}$) respectively
234 averaged to 38 (1.2–263) ng m^{-3} and 0.25 (0.03–0.86) %. $\sum 9\text{NACs}$ and $\sum 9\text{NACs}/\text{OM}$
235 respectively averaged 53 (4.5–263) ng m^{-3} and 0.33 (0.09–0.86) % during heating, both
236 values are two times higher in magnitude in comparison to those measured before
237 heating (averaged 20 (1.2–108) ng m^{-3} and 0.15 (0.03–0.4) %, respectively). $\sum 9\text{NACs}$
238 exhibited a nighttime increase, reaching approximately twice the levels observed during
239 daytime throughout the entire campaign (Fig. 3a). The observed difference between day
240 and night is consistent with our previous research (Ren et al., 2022). However, the
241 relative molecular composition of the total nine NACs in $\text{PM}_{2.5}$ did not manifest any
242 significant change (Fig. 4a, c), 4-Nitrophenol (4NP) was found to have the highest
243 concentration among all species, accounting for 44% and 42% of the total NACs before
244 and during heating, followed by 4-nitrocatechol (4NC) which accounted for 21% before
245 heating and 23% during heating. These findings align with the dominant species
246 observed in previous studies (Ren et al., 2022; Ren et al., 2023; Li et al., 2020) however
247 the values were much higher in comparison to those found in our earlier work (Ren et
248 al., 2022) at the same sample site during the spring (8.6 (0.48–27) ng m^{-3}) and summer
249 (8.5 (1.0–16) ng m^{-3}). It's plausible that seasonal variations in NACs are linked to
250 emission sources, formation pathways, and weather conditions. In this study, the overall
251 abundance of the $\sum 9\text{NACs}$ appeared to align closely with measurements from earlier



252 studies conducted during winter in Beijing ($74 \pm 51 \text{ ng m}^{-3}$ in winter, $20 \pm 12 \text{ ng m}^{-3}$ in
 253 autumn) (Li et al., 2020) and Jinan ($48 \pm 26 \text{ ng m}^{-3}$ in winter, $9.8 \pm 4.2 \text{ ng m}^{-3}$ in autumn,) (Wang et al., 2018), but are significantly higher than those measured for Xi'an (17 ± 12
 254 ng m^{-3}) and Hong Kong ($12 \pm 14 \text{ ng m}^{-3}$) in winter (Wu et al., 2020; Chow et al., 2015).
 255
 256 In contrast to studies conducted abroad, the levels of $\Sigma 9\text{NACs}$ in this particular study
 257 tended to be higher Germany showed 16 ng m^{-3} , while in the UK, levels were around
 258 19 ng m^{-3} . Belgium recorded levels of 32 ng m^{-3} in winter and 13 ng m^{-3} in autumn.
 259 (Teich et al., 2017; Mohr et al., 2013; Kahnt et al., 2013). This indicates that it is urgent
 260 to further reduce the concentration of contaminant precursors in China.

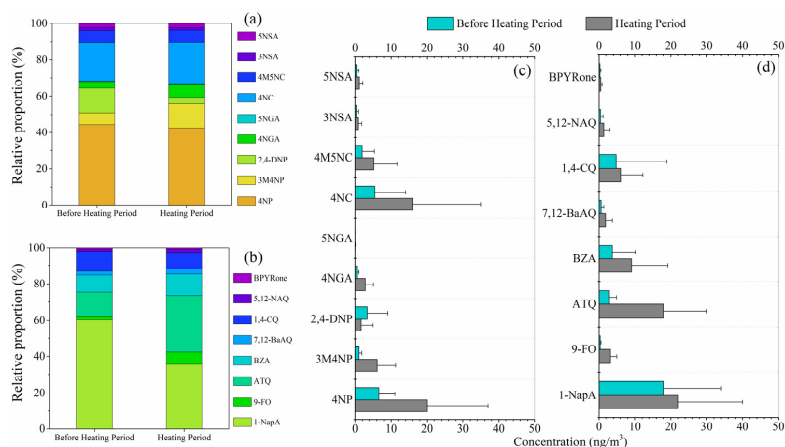


261
 262 Fig.3 NACs and OPAHs concentrations (a,b) and contributions of secondary
 263 formation (SNACs, SOPAHs) to the total (c) before and during heating periods.

264 Throughout the sampling, the total concentrations of OPAHs ($\Sigma 8\text{OPAHs}$)
 265 averaged $47 (1.2\text{--}234) \text{ ng m}^{-3}$ whereas the mean value for their total contribution to OM
 266 ($\Sigma 8\text{OPAHs}/\text{OM}$) was $0.33 (0.06\text{--}0.81) \%$ (Table S1). These values were both slightly
 267 higher than those of NACs in this work. $\Sigma 8\text{OPAHs}$ and $\Sigma 8\text{OPAHs}/\text{OM}$ respectively
 268 averaged $61 (6.9\text{--}218) \text{ ng m}^{-3}$ and $0.40 (0.18\text{--}0.58) \%$ during heating. These values are
 269 almost twice as much as those measured before heating (averaging $31 (2.1\text{--}234) \text{ ng m}^{-3}$
 270 3 and $0.24 (0.06\text{--}0.81) \%$, respectively). Like the $\Sigma 9\text{NACs}$, the combined levels of



271 Σ 8OPAHs were higher during nighttime compared to daytime, averaging about twice
 272 as high before heating and 1.3 times during heating, as indicated in Fig. 3b. Among the
 273 eight OPAHs studied, 1-NapA constituted the highest proportion before (60%) and
 274 during (36%) heating. However, the relative proportion of ATQ more than doubled,
 275 increasing from 13% before heating to 31% during heating, as depicted in Fig. 4b and
 276 d. The average concentrations of Σ 8OPAHs were higher than those recorded for other
 277 Chinese urban sites, including Guangzhou (23 ng m⁻³) and Xi'an (54 ng m⁻³) (Ren et
 278 al., 2017) as well as higher than those documented for the south (41.8 ng m⁻³, traffic
 279 site) (Alves et al., 2017) and central (~10 ng m⁻³) European cities (Lammel et al., 2020).
 280 The average concentrations of Σ 8OPAHs were also higher than those recorded for
 281 Mainz, Germany (0.047-1.6 ng m⁻³) and Thessaloniki, Greece (0.86-4.3 ng m⁻³)
 282 (Kitanovski et al., 2020).



283

284 Fig.4 Comparison of measurements before and during the heating period at the urban
 285 site of Beijing, including (a) Relative proportion of NAC species, (b) Relative
 286 proportion of OPAH species, (c) NAC concentrations, and (d) OPAH concentrations.
 287 (4NP: 4-nitrophenol, 3M4NP: 3-methyl-4-nitrophenol, 2, 4-DNP: 2,4-dinitrophenol,
 288 4NGA: 4-nitroguaiacol, 5NGA: 5-nitroguaiacol, 4NC: 4-nitrocatechol, 4M5NC: 4-



289 methyl-5-nitrocatechol, 3NSA: 3-nitro-salicylic acid, 5NSA: 5-nitro-salicylic acid; 1-
290 NapA: 1-Naphthaldehyde, 9-FO: 9-fluorenone, ATQ: anthraquinone, BZA:
291 benzanthrone, 7,12-BaAQ: benzo(a)anthracene-7,12-dione, 1,4-CQ: 1,4-
292 chrysenequinone, 5,12-NAQ: 5,12-naphthacenequinone, and BPYRone: 6H-
293 benzo(cd)pyrene-6-one)

294 **3.3 Sources and formation of BrC compounds**

295 The relation between individual and total species and the associated pollutants—
296 levoglucosan, K^+ , SO_2 , NO_2 , O_3 , RH, and SIA—was examined according to the data
297 findings for the Pearson correlations shown in Table 2 (for NACs) and Table 3 (for
298 OPAHs) to provide additional clarity regarding the source and formation of NACs and
299 OPAHs. The strong correlations observed throughout the entire campaign between
300 levoglucosan (an organic tracer associated with biomass burning), K^+ (an inorganic
301 tracer linked to biomass burning), and NO_2 with total NACs and all identified NAC
302 species indicate that both automobile emissions and biomass burning played significant
303 roles in the accumulation of NACs in urban Beijing during autumn and winter. The
304 correlation between NACs and SO_2 was significantly higher during heating ($r=0.275$,
305 $p<0.05$) compared to pre-heating, indicating that coal combustions play a more
306 significant role in NAC formation after heating commences.

307 In addition to these primary pollutants, NACs were also significantly correlated
308 with some secondary pollutants. Before heating, there existed a strong positive
309 association ($r=0.692$, $p<0.01$) between NACs and O_3 . However, this association
310 changed considerably after heating, becoming notably negative ($r=-0.303$, $p<0.05$).
311 NACs and RH concurrently displayed a strong positive correlation ($r=0.548$, $p<0.01$)



312 during heating. Along with SO_4^{2-} , NO_3^- , and NH_4^+ total NACs also exhibited high
313 positive correlation, particularly while heating ($r=0.373$, $p<0.01$; $r=0.504$, $p<0.01$;
314 $r=0.513$, $p<0.01$, respectively). The overall concentrations of OPAHs and NACs
315 throughout the campaign exhibited substantial correlations ($r=0.830$, $p<0.01$ before
316 heating; $r=0.895$, $p<0.01$ during heating) (Table 3, Fig. S1). This suggests that their
317 sources and/or influencing variables were comparable. Specifically, throughout the
318 entire campaign, both total OPAHs and all identified OPAH species exhibited a strong
319 correlation with levoglucosan, K^+ , and NO_2 . This implies that automobile emissions
320 and biomass burning played significant roles as sources of OPAHs. OPAHs and SO_2
321 ($r=0.365$, $p<0.01$) were determined to be more strongly correlated during heating than
322 before heating, suggesting the contribution of coal combustions to OPAHs becomes
323 significant when heating begins. Moreover, the correlation between OPAHs and O_3 was
324 significantly positive before heating ($r=0.563$, $p<0.01$), whereas it was significantly
325 negative during heating ($r=-0.385$, $p<0.01$). Furthermore, it was discovered that
326 throughout the heating phase, OPAHs and RH had a substantial positive correlation
327 ($r=0.578$, $p<0.01$). Total OPAHs also showed good correlations with SO_4^{2-} , NO_3^- , and
328 NH_4^+ , especially during heating period ($r=0.477$, $p<0.01$; $r=0.658$, $p<0.01$; $r=0.658$,
329 $p<0.01$; respectively).

330 The observed phenomena, involving photooxidation before heating and aqueous
331 reactions during heating, strongly suggest a significant role in the secondary creation
332 of BrC throughout the entire sampling period. Earlier studies have highlighted that in
333 certain regions, the primary mechanism driving the formation of nitro-aromatic



334 hydrocarbons involves the gaseous phase oxidation of VOC precursors from
 335 anthropogenic sources, such as toluene and benzene (Olariu et al., 2002; Sato et al.,
 336 2007; Yuan et al., 2016; Ji et al., 2017; Liu et al., 2023). According to a recent study,
 337 for instance, NACs are mostly generated at a rural location on China's Chongming
 338 Island through gaseous-phase photooxidation (Liu et al., 2023). Aqueous reaction is
 339 also a key pathway for the formation of BrC (Zhang et al., 2020; Cheng et al., 2021;
 340 Jiang et al., 2023). Zhang et al., suggested that the aqueous formation of anthropogenic
 341 secondary organic carbon was a key source of atmospheric BrC in Xi'an (Zhang et al.,
 342 2020). Wang et al.'s field observations in urban Beijing revealed that the aqueous
 343 reaction is a significant mechanism for the secondary synthesis of nitro-aromatic
 344 hydrocarbons during summer temperatures with high relative humidity (Wang et al.,
 345 2019).

346

Table 2 Correlations between NACs and meteorological parameters, gas pollutants, and aerosol components before (n=56) and during the heating period (n=66).

	Before heating period	levoglucosan	K ⁺	SO ₂	NO ₂	O ₃	RH	SO ₄ ²⁻	NO ₃ ⁻	NH ₄ ⁺
NACs	∑9NACs	0.897**	0.738**	0.210	0.714**	0.692**	0.170	0.359**	0.369**	0.190
	4NP	0.784**	0.699**	0.249	0.715**	0.649**	0.118	0.345**	0.372**	0.207
	3M4NP	0.752**	0.526**	0.290*	0.575**	0.511**	-0.011	0.184	0.191	0.029
	2,4-DNP	0.436**	0.353**	0.310*	0.463**	0.492**	-0.151	0.034	-0.048	-0.166
	4NGA	0.545**	0.361**	0.438**	0.560**	0.524**	-0.137	-0.016	-0.025	-0.131
	5NGA	0.582**	0.355**	0.114	0.343**	0.433**	0.005	0.120	0.139	0.044
	4NC	0.897**	0.748**	0.064	0.641**	0.617**	0.308*	0.448**	0.486**	0.325*
	4M5NC	0.885**	0.668**	0.076	0.579**	0.577**	0.252	0.364**	0.413**	0.261
	3NSA	0.791**	0.678**	0.129	0.553**	0.495**	0.214	0.457**	0.515**	0.331*
	5NSA	0.737**	0.596**	0.219	0.594**	0.553**	0.085	0.279*	0.316*	0.125
	During heating period	levoglucosan	K ⁺	SO ₂	NO ₂	O ₃	RH	SO ₄ ²⁻	NO ₃ ⁻	NH ₄ ⁺
NACs	∑9NACs	0.888**	0.786**	0.275*	0.481**	-0.303*	0.548**	0.373**	0.504**	0.513**
	4NP	0.812**	0.725**	0.262*	0.471**	-0.296*	0.586**	0.390**	0.489**	0.511**
	3M4NP	0.756**	0.655**	0.248	0.374**	-0.225	0.613**	0.318**	0.397**	0.462**



2,4-DNP	0.537**	0.495**	0.280*	0.417**	-0.304*	0.199	0.136	0.247*	0.136
4NGA	0.672**	0.406**	0.229	0.274*	-0.206	0.201	-0.047	0.074	0.081
5NGA	0.275*	0.208	-0.028	0.190	0.026	-0.006	0.114	0.100	0.125
4NC	0.894**	0.804**	0.248	0.454**	-0.290*	0.520**	0.378**	0.523**	0.530**
4M5NC	0.882**	0.736**	0.246	0.434**	-0.244	0.430**	0.283*	0.421**	0.422**
3NSA	0.788**	0.910**	0.348**	0.681**	-0.410**	0.577**	0.707**	0.888**	0.828**
5NSA	0.820**	0.866**	0.268*	0.629**	-0.377**	0.599**	0.680**	0.846**	0.828**

**significant correlation at the 0.01 level;

*significant correlation at the 0.05 level;

347 From the above analysis, it is evident that there is a good correlation between these
 348 two aromatic compounds and levoglucosan, as well as SO₂. Since levoglucosan and
 349 SO₂ are long-lived and inert chemicals in the atmosphere (Cai et al., 2022), it was not
 350 possible to determine with certainty whether NACs and OPAHs originated
 351 predominantly from direct emission from the coal and biomass combustion or by
 352 secondary oxidation of the precursors produced as a result of these processes. Equations
 353 1 and 2's outcomes indicated that in Beijing's urban areas during fall and winter, NACs
 354 and OPAHs were predominantly of secondary origin. Throughout the entire sampling
 355 period, secondary formation accounted for 17% to 99% (average of 80%) of NACs and
 356 8.9% to 99% (average of 73%) of OPAHs, as depicted in Fig. 3c. Notably, the secondary
 357 fraction for OPAHs increased by 10.4% from 86% to 96%, while the secondary fraction
 358 for NACs rose by 8.9% from 90% before heating to 98% during heating. Earlier studies
 359 have highlighted the presence of significant levels of secondary particle BrC during
 360 autumn and winter, particularly during haze periods (Ding et al., 2017; Liu et al., 2023),
 361 and the results of this work corroborate well with the earlier studies. Moreover, the good
 362 correlations between OPAHs and NACs with O₃ before heating and with RH during
 363 heating, confirm the importance of photochemical and aqueous oxidation in these two



364 different periods.

365

Table 3 Correlations between OPAHs and meteorological parameters, gas pollutants, and aerosol components before (n=56) and during the heating period (n=66).

Before heating period	Σ 9NACs	levoglucosan	K ⁺	SO ₂	NO ₂	O ₃	RH	SO ₄ ²⁻	NO ₃ ⁻	NH ₄ ⁺
Σ 8OPAHs	0.830**	0.865**	.605**	0.188	0.563**	0.563**	0.143	0.244	0.283*	0.139
1-NapA	0.844**	0.870**	.621**	0.211	0.640**	0.622**	0.174	0.213	0.238	0.096
9-FO	0.775**	0.785**	.646**	0.283*	0.558**	0.573**	0.059	0.183	0.235	0.119
ATQ	0.633**	0.694**	.497**	0.392**	0.477**	0.483**	-0.018	0.042	0.061	-0.024
OPAHs BZA	0.686**	0.759**	.573**	0.232	0.537**	0.594**	0.110	0.177	0.206	0.117
7,12-BaAQ	0.821**	0.865**	.685**	0.189	0.591**	0.622**	0.187	0.325*	0.356**	0.224
1,4-CQ	0.636**	0.646**	.406**	0.041	0.303*	0.290*	0.102	0.259	0.309*	0.174
5,12-NAQ	0.694**	0.752**	.563**	0.227	0.511**	0.559**	0.091	0.184	0.214	0.110
BPYRone	0.827**	0.870**	.662**	0.131	0.590**	0.616**	0.226	0.345**	0.398**	0.255
Heating period	Σ 9NACs	levoglucosan	K ⁺	SO ₂	NO ₂	O ₃	RH	SO ₄ ²⁻	NO ₃ ⁻	NH ₄ ⁺
Σ 8OPAHs	0.895**	0.931**	0.877**	0.365**	0.678**	-0.385**	0.578**	0.477**	0.658**	0.658**
1-NapA	0.752**	0.774**	0.659**	0.248	0.547**	-0.378**	0.332*	0.332**	0.498**	0.446**
9-FO	0.478**	0.457**	0.342**	0.305*	0.302*	-0.020	0.131	-0.013	0.167	0.250*
ATQ	0.780**	0.797**	0.815**	0.426**	0.668**	-0.372**	0.656**	0.466**	0.642**	0.684**
OPAHs BZA	0.840**	0.881**	0.829**	0.332**	0.570**	-0.273*	0.577**	0.431**	0.568**	0.577**
7,12-BaAQ	0.801**	0.856**	0.896**	0.391**	0.633**	-0.299*	0.655**	0.531**	0.689**	0.710**
1,4-CQ	0.703**	0.780**	0.791**	0.244	0.597**	-0.282*	0.624**	0.560**	0.647**	0.675**
5,12-NAQ	0.777**	0.818**	0.869**	0.365**	0.601**	-0.293*	0.535**	0.444**	0.619**	0.614**
BPYRone	0.858**	0.857**	0.845**	0.339**	0.588**	-0.320*	0.478**	0.396**	0.612**	0.568**

**significant correlation at the 0.01 level;

*significant correlation at the 0.05 level;

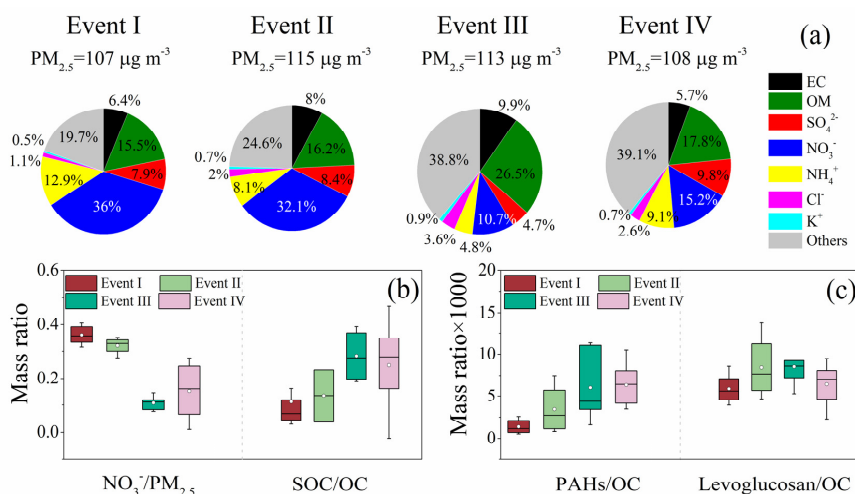
366

367 3.4 Different pollution characteristics in haze events

368 From Fig.1, it can be found that PM_{2.5} shows four equivalent maxima lasting for
 369 two to five days. Among the four pollution events, two occurred before heating (24-27,
 370 October and 5-6, November) and the other two occurred during heating (18-20,
 371 November and 27-31 December). PM_{2.5} was significantly different in terms of its
 372 chemical constituents before and during heating although the mass concentration of



373 $PM_{2.5}$ was rather similar (respectively averaging 107, 115, 113, and 108 $\mu\text{g m}^{-3}$ for
374 Event I, II, III, and IV) (Fig. 5a). In the two events before heating, OM existed as the
375 second most dominant species in $PM_{2.5}$, with the respective relative abundance of 15.5%
376 and 16.2% in Events I and II. In contrast, OM surfaced as the most dominant species of
377 $PM_{2.5}$ during heating. The relative abundance of OM (26.5%) during Event III was
378 higher (17.8%) than that during Event IV (Fig.5a). The ratios of $\text{NO}_3^-/PM_{2.5}$ were higher
379 in Events I and II as compared to Events III and IV, with the ratios of SOC/OC showing
380 the opposite trend (Fig.5b), suggesting a significant increase in the concentration of
381 secondary organic compounds after heating. In the context of fossil fuel combustion,
382 PAHs serve as markers for coal burning, while levoglucosan acts as a significant tracer
383 for biomass smoke. Figure 5c shows that the ratios of PAHs to organic carbon mass in
384 $PM_{2.5}$ (PAHs/OC) were higher during Events III and IV compared to Events I and II.
385 This underscores the heightened emissions from household burning of coal for heating
386 purposes. Levoglucosan/OC, the mass ratio of levoglucosan to OC in $PM_{2.5}$, did not,
387 however, rise considerably over the same period (Fig. 5c), indicating a similar degree
388 of emissions from burning biomass before and during heating. This result was
389 consistent with our earlier research from the 2014 APEC meeting (Wang et al., 2017).



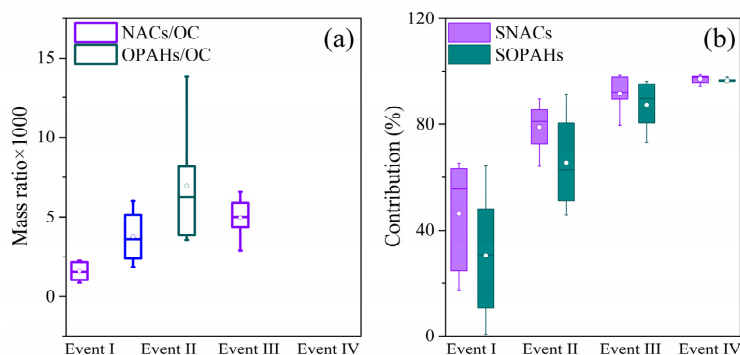
390

391 Fig.5 Comparative analysis of the chemical composition of PM_{2.5} during four distinct
 392 events of air pollution. (a) Relative percentages of major species in PM_{2.5}; (b, c) mass
 393 ratios of the key species and organic tracers in PM_{2.5}.

394 According to the majority of research, Beijing's haze is distinguished by intense
 395 secondary formation (Zhang et al., 2018; Xu et al., 2017; Sun et al., 2016; Guo et al.,
 396 2014). According to several research studies, organic materials (OM) predominates in
 397 the autumn and winter, while secondary SIA is the most prevalent species in the
 398 summer (Renhe et al., 2014). Additionally, according to a few investigators, SIA has a
 399 major role in wintertime pollution episodes (Guo et al., 2014; Wang et al., 2016).
 400 Furthermore, a recent investigation identified the species responsible for Beijing haze,
 401 and listed distinct haze-driving species operative over the year: The haze is primarily
 402 OM-driven during winter and late fall, nitrate-driven in early fall, sulfate-driven in
 403 summer, whereas it is driven primarily by nitrates during spring (Tan et al., 2018). Table
 404 4 and Fig.5a depict that PM_{2.5} was enriched with SIA especially NO₃⁻ during Events I
 405 and II, but enriched OM with higher levels of SOC was observed during Events III and
 406 IV. The findings strongly indicated that haze during fall and winter in urban Beijing



407 was primarily influenced by nitrate before heating and shifted to being driven by SOC
408 during heating. Table 4 illustrates that T (temperature) and RH (relative humidity) were
409 notably higher during Events I and II compared to Events III and IV. These warmer and
410 moister conditions favored photochemical oxidation, leading to an increased abundance
411 of SIA during the same period. Home heating activities, such as burning residential coal,
412 were increased during the heating period. This resulted in massive emissions of SO₂,
413 NO_x, VOCs, and primary particles, all of which were conducive to the generation of
414 SOC. As a result, during Events III and IV, SOC concentrations and relative
415 abundances were higher than during Events I and II. Furthermore, Fig. 6a shows that
416 the NACs/OC and OPAHs/OC ratios were significantly higher in Events III and IV
417 compared to Events I and II. Figure 6b displays a parallel trend in the relative
418 contributions of secondary formation for both events, highlighting a notable increase in
419 the secondary formation of BrC during pollution events, particularly evident during
420 heating periods.



421
422 Fig. 6 Comparative analysis of the chemical composition of BrC during four distinct
423 air pollution events. (a) Mass ratios of NACs and OPAHs to OC in PM_{2.5}. (b) Relative
424 contributions of secondary formation (SNACs/OPAHs) to the total NACs/OPAHs in
425 the fine particulate.



426

Table 4. Meteorological parameters, chemical components ($\mu\text{g m}^{-3}$) of $\text{PM}_{2.5}$, and concentrations of gaseous pollutants (ppb) among four pollution episodes in Beijing.

	Before Heating Period		During Heating Period	
	Event I 24/10–27/10 <i>N</i> =8	Event II 5/11–6/11 <i>N</i> =4	Event III 18/11–20/11 <i>N</i> =6	Event IV 27/12–31/12 <i>N</i> =10
$\text{PM}_{2.5}$	107 ± 29	115 ± 48	113 ± 37	108 ± 35
Temperature, °C	13 ± 1.6	8.8 ± 4.2	1.8 ± 2.6	1.8 ± 3.8
Relative humidity, %	79 ± 10	55 ± 26	29 ± 10	36 ± 22
SO_2	1.4 ± 0.1	1.9 ± 1.1	5.0 ± 1.0	4.0 ± 1.2
NO	27 ± 19	27 ± 15	51 ± 42	47 ± 31
NO_2	30 ± 6.7	33 ± 14	40 ± 12	37 ± 8.1
SIA ^a	62 ± 20	58 ± 22	23 ± 9.9	39 ± 30
NO_3^-	39 ± 13	38 ± 15	12 ± 5.2	18 ± 14
SOC ^b	1.9 ± 1.3	2.3 ± 1.8	7.0 ± 2.8	3.9 ± 2.5
NACs (ng m^{-3})	17 ± 8.3	41 ± 36	131 ± 85	55 ± 27
OPAHs (ng m^{-3})	21 ± 7.6	62 ± 85	127 ± 53	74 ± 23

^a SIA: secondary inorganic aerosols (the sum of sulfate, nitrate, and ammonium).

^b SOC: secondary organic carbon ($[\text{SOC}] = [\text{OC}] - [\text{EC}] \times ([\text{OC}]/[\text{EC}]_{\text{pri}})$). $[\text{OC}]/[\text{EC}]_{\text{pri}}$ was estimated from the fitting of the minimum $[\text{OC}]/[\text{EC}]$ ratio, assuming that the primary source dominated the period with minimal secondary formation. In this work, $([\text{OC}]/[\text{EC}])_{\text{pri}}$ was estimated from the fitting of the lowest 15% $[\text{OC}]/[\text{EC}]$ ratios during the whole sampling period.

427 4 Conclusions

428 The current study determined the concentrations of $\text{PM}_{2.5}$ -bound nine NACs and
 429 eight OPAHs in autumn and winter in Beijing urban areas. The OPAHs and NACs
 430 concentrations were much higher during heating than before heating. These species
 431 have a distinct diurnal variation, with higher concentrations at night compared to day.
 432 4-Nitrophenol, 4-nitrocatechol, and 1-Naphthaldehyde were the most abundantly
 433 existing species in the whole campaign.

434 The primary sources of NACs and OPAHs were biomass combustion and
 435 automobile emissions, with the secondary generation of BrC being the predominant



436 contributor across the entire sampling period. Our results underscore the significant role
437 of secondary generation in producing BrC, particularly its heightened contribution
438 during pollution events linked to heating. A comparative analysis of the chemical
439 constitution of PM_{2.5} and BrC in four different haze events also revealed that the haze
440 in the autumn and winter was caused by SOC during heating and by nitrate prior to
441 heating. Increased attention should be directed towards reducing the emissions of
442 aromatic hydrocarbons and other anthropogenic volatile organic compounds (VOCs)
443 when heating commences. This focus is crucial for effectively mitigating pollution and
444 ensuring the preservation of human health. There is still only a limited volume of
445 research on the molecular makeup of BrC, with this study primarily concentrating on
446 two chromophores. As a result, further research is needed to identify more impactful
447 chromophores at a molecular level. Additionally, a comprehensive exploration of the
448 secondary generation pathways and key influencing factors of BrC through field
449 observations and laboratory simulations is essential. This investigation is crucial for
450 accurately assessing the environmental and human health impacts of BrC.

451 **Data availability**

452 The field observational and the lab experimental data used in this study are
453 available from the corresponding author upon request (Hong Li via
454 lihong@craes.org.cn).



455 **Author contributions**

456 Yanqin Ren, Gehui Wang and Hong Li designed the research; Yanqin Ren,
457 Yuanyuan Ji and Zhenhai Wu collected the samples; Yanqin Ren, Fang Bi and Hao
458 Zhang conducted the experiments; Yanqin Ren and Gehui Wang analyzed the data,
459 Yanqin Ren wrote the paper; Gehui Wang, Junling Li, Haijie Zhang and Hong Li
460 contributed to the paper with useful scientific discussions and comments.

461 **Competing interests**

462 The authors declare that they have no conflict of interest.

463 **Acknowledgements**

464 This work was supported by the Fundamental Research Funds for Central Public
465 Welfare Scientific Research Institutes of China (No. 2022YSKY-27; No. 2019YSKY-
466 018), and the National Natural Science Foundation of China (No. 42130704; No.
467 41907197).

468 **References**

469 Alves, C., Vicente, A., CustÃ³dio, D., Cerqueira, M., Nunes, T., Pio, C., Lucarelli, F., Calzolari, G., Nava,
470 S., and Diapouli, E.: Polycyclic aromatic hydrocarbons and their derivatives (nitro-PAHs,
471 oxygenated PAHs, and azaarenes) in PM_{2.5} from Southern European cities, *Sci. Total. Environ.*,
472 595, 494-504, <http://dx.doi.org/10.1016/j.scitotenv.2017.03.256>, 2017.
473 Bai, X., Wei, J., Ren, Y., Gao, R., Chai, F., Li, H., Xu, F., and Kong, Y.: Pollution characteristics and
474 health risk assessment of Polycyclic aromatic hydrocarbons and Nitrated polycyclic aromatic



- 475 hydrocarbons during heating season in Beijing, *JEnvS*, 123, 169-182,
476 <https://doi.org/10.1016/j.jes.2022.02.047>, 2023.
- 477 Cai, D., Wang, X., George, C., Cheng, T., Herrmann, H., Li, X., and Chen, J.: Formation of Secondary
478 Nitroaromatic Compounds in Polluted Urban Environments, *J. Geophys. Res.-Atmos.*,
479 <https://doi.org/10.1029/2021JD036167>, 2022.
- 480 Cheng, X., Chen, Q., Li, Y., Huang, G., Liu, Y., Lu, S., Zheng, Y., Qiu, W., Lu, K., Qiu, X., Bianchi, F.,
481 Yan, C., Yuan, B., Shao, M., Zhe Wang, R. M., Canagaratna, Zhu, T., Wu, Y., and Zeng, L.:
482 Secondary Production of Gaseous Nitrated Phenols in Polluted Urban Environments, *Environ.*
483 *Sci. Technol.*, 55, 4410-4419, <https://doi.org/10.1021/acs.est.0c07988>, 2021.
- 484 Chow, K. S., Huang, X. H. H., and Yu, J. Z.: Quantification of nitroaromatic compounds in atmospheric
485 fine particulate matter in Hong Kong over 3 years: field measurement evidence for secondary
486 formation derived from biomass burning emissions, *Environmental Chemistry*, 13, 665,
487 <https://doi.org/10.1071/EN15174>, 2015.
- 488 Claeys, M., Vermeylen, R., Yasmeeen, F., Gómez-González, Y., Chi, X., Maenhaut, W., Mészáros, T., and
489 Salma, I.: Chemical characterisation of humic-like substances from urban, rural and tropical
490 biomass burning environments using liquid chromatography with UV/vis photodiode array
491 detection and electrospray ionisation mass spectrometry, *Environmental Chemistry*, 9, 273-284,
492 <http://dx.doi.org/10.1071/EN11163>, 2012.
- 493 Ding, X., Zhang, Y. Q., He, Q., Yu, Q. Q., Wang, J. Q., Shen, R. Q., Song, W., Wang, Y., and Wang, X.:
494 Significant increase of aromatics-derived secondary organic aerosol during fall to winter in
495 China, *Environ. Sci. Technol.*, 13, 7432-7441, <http://doi.org/10.1021/acs.est.6b06408>, 2017.
- 496 Du, Z., He, K., Cheng, Y., Duan, F., Ma, Y., Liu, J., Zhang, X., Zheng, M., and Weber, R.: A yearlong
497 study of water-soluble organic carbon in Beijing II: Light absorption properties, *Atmos.*
498 *Environ.*, 89, 235-241, <http://doi.org/10.1016/j.atmosenv.2014.02.022>, 2014.
- 499 Fan, Xingjun, Peng, Ping'an, Song, and Jianzhong: Temporal variations of the abundance and optical
500 properties of water soluble Humic-Like Substances (HULIS) in PM_{2.5} at Guangzhou, China,
501 *Atmos. Res.*, <http://doi.org/10.1016/j.atmosres.2015.12.024>, 2016.
- 502 Finewax, Zachary, de, Gouw, Joost, A., Ziemann, Paul, and J.: Identification and Quantification of 4-
503 Nitrocatechol Formed from OH and NO₃ Radical-Initiated Reactions of Catechol in Air in the
504 Presence of NO_x: Implications for Secondary Organic Aerosol Formation from Biomass
505 Burning, *Environ. Sci. Technol.*, <http://doi.org/10.1021/acs.est.7b05864> 2018.
- 506 Guo, S., Hu, M., Zamora, M. L., Peng, J., Shang, D., Zheng, J., Du, Z., Wu, Z., Shao, M., and Zeng, L.:
507 Elucidating severe urban haze formation in China, *Proc. Natl. Acad. Sci. USA.*, 111, 17373-
508 17378, <http://doi.org/10.1073/pnas.1419604111>, 2014.
- 509 Huang, R. J., Yang, L., Cao, J., Chen, Y., Chen, Q., Li, Y., Duan, J., Zhu, C., Dai, W., Wang, K., Lin, C.,
510 Ni, H., Corbin, J. C., Wu, Y., Zhang, R., Tie, X., Hoffmann, T., O'Dowd, C., and Dusek, U.:
511 Brown Carbon Aerosol in Urban Xi'an, Northwest China: The Composition and Light
512 Absorption Properties, *Environ. Sci. Technol.*, 52, 6825-6833,
513 <http://doi.org/10.1021/acs.est.8b02386>, 2018.
- 514 Iinuma, Y., Boge, O., Graefe, R., and Herrmann, H.: Methyl-Nitrocatechols: Atmospheric Tracer
515 Compounds for Biomass Burning Secondary Organic Aerosols, *Environ. Sci. Technol.*, 44, 8453,
516 <http://doi.org/10.1021/es102938a>, 2010.
- 517 Ji, Y., Zhao, J., Terazono, H., Misawa, K., and Zhang, R.: Reassessing the atmospheric oxidation



- 518 mechanism of toluene, Proc Natl Acad Sci U S A, 114, <http://doi.org/10.1073/pnas.1705463114>,
519 2017.
- 520 Jiang, H., Cai, J., Feng, X., Chen, Y., Wang, L., Li, J., Tang, J., Mo, Y., Zhang, X., Zhang, G., Mu, Y.,
521 and Chen, J.: Aqueous-Phase Secondary Processes and Meteorological Change Promote the
522 Brown Carbon Formation and Transformation During Haze Events, J. Geophys. Res.-Atmos.,
523 <http://doi.org/10.1029/2023JD038735>, 2023.
- 524 Kahnt, A., Behrouzi, S., Vermeylen, R., Shalamzari, M. S., Vercauteren, J., Roekens, E., Claeys, M., and
525 Maenhaut, W.: One-year study of nitro-organic compounds and their relation to wood burning
526 in PM10 aerosol from a rural site in Belgium, Atmos. Environ., 81, 561-568,
527 <http://dx.doi.org/10.1016/j.atmosenv.2013.09.041>, 2013.
- 528 Kitanovski, Z., Shahpoury, P., Samara, C., Voliotis, A., and Lammel, G.: Composition and mass size
529 distribution of nitrated and oxygenated aromatic compounds in ambient particulate matter from
530 southern and central Europe – implications for the origin, Atmos. Chem. Phys., 20, 2471-2487,
531 <https://doi.org/10.5194/acp-20-2471-2020>, 2020.
- 532 Lammel, G., Kitanovski, Z., Kukucka, P., Novák, J., and Wietzoreck, M.: Oxygenated and nitrated
533 polycyclic aromatic hydrocarbons (OPAHs, NPAHs) in ambient air - levels, phase partitioning,
534 mass size distributions and inhalation bioaccessibility, Environ. Sci. Technol., 54, 2615-2625,
535 <https://dx.doi.org/10.1021/acs.est.9b06820>, 2020.
- 536 Laskin, A., Laskin, J., and Nizkorodov, S. A.: Chemistry of atmospheric brown carbon, Chem. Rev., 115,
537 4335-4382, <http://doi.org/10.1021/cr5006167>, 2015.
- 538 Li, J., Wang, G., Ren, Y., Wang, J., Wu, C., Han, Y., Zhang, L., Cheng, C., and Meng, J.: Identification
539 of chemical compositions and sources of atmospheric aerosols in Xi'an, inland China during
540 two types of haze events, Sci. Total. Environ., 566, 230-237,
541 <http://dx.doi.org/10.1016/j.scitotenv.2016.05.057>, 2016.
- 542 Li, X., Yang, Y., Liu, S., Zhao, Q., Wang, G., and Wang, Y.: Light absorption properties of brown carbon
543 (BrC) in autumn and winter in Beijing: Composition, formation and contribution of nitrated
544 aromatic compounds, Atmos. Environ., 223, 117289,
545 <https://doi.org/10.1016/j.atmosenv.2020.117289>, 2020.
- 546 Li, X., Han, J., Hopke, P. K., Hu, J., Shu, Q., Chang, Q., and Ying, Q.: Quantifying primary and secondary
547 humic-like substances in urban aerosol based on emission source characterization and a source-
548 oriented air quality model, Copernicus GmbH, <https://doi.org/10.5194/acp-19-2327-2019>, 2019.
- 549 Li, Y., Bai, X., Ren, Y., Gao, R., Ji, Y., Wang, Y., and Li, H.: PAHs and nitro-PAHs in urban Beijing from
550 2017 to 2018: Characteristics, sources, transformation mechanism and risk assessment, J.
551 Hazard. Mater., 436, 1-11, <https://doi.org/10.1016/j.jhazmat.2022.129143>, 2022.
- 552 Liu, J., Mo, Y., Ding, P., Li, J., Shen, C., and Zhang, G.: Dual carbon isotopes (¹⁴C and ¹³C) and optical
553 properties of WSOC and HULIS-C during winter in Guangzhou, China, Sci. Total. Environ.,
554 633, 1571-1578, <https://doi.org/10.1016/j.scitotenv.2018.03.293>, 2018.
- 555 Liu, X., Wang, H., Wang, F., Lv, S., Wu, C., Zhao, Y., Zhang, S., Liu, S., Xu, X., Lei, Y., and Wang, G.:
556 Secondary Formation of Atmospheric Brown Carbon in China Haze: Implication for an
557 Enhancing Role of Ammonia, Environ. Sci. Technol., <http://doi.org/10.1021/acs.est.3c03948>,
558 2023.
- 559 Lu, C., Wang, X., Dong, S., Zhang, J., and Wang, W.: Emissions of fine particulate nitrated phenols from
560 various on-road vehicles in China, Environ. Res., 179, 108709,



- 561 <https://doi.org/10.1016/j.envres.2019.108709>, 2019a.
- 562 Lu, C., Wang, X., Li, R., Gu, R., Zhang, Y., Li, W., Gao, R., Chen, B., Xue, L., and Wang, W.: Emissions
563 of fine particulate nitrated phenols from residential coal combustion in China, *Atmos. Environ.*,
564 203, 10-17, <https://doi.org/10.1016/j.atmosenv.2019.01.047>, 2019b.
- 565 Ma, Y., Cheng, Y., Qiu, X., Cao, G., Fang, Y., Wang, J., Zhu, T., Yu, J., and Hu, D.: Sources and oxidative
566 potential of water-soluble humic-like substances (HULISWS) in fine particulate matter (PM_{2.5})
567 in Beijing, *Atmos. Chem. Phys.*, 18, 5607–5617, <https://doi.org/10.5194/acp-18-5607-2018>,
568 2018.
- 569 Mohr, C., Lopez-Hilfiker, F. D., Zotter, P., A. S. H. P., Xu, L., Ng, N. L., Herndon, S. C., Williams, L.
570 R., Franklin, J. P., Zahniser, M. S., Worsnop, D. R., Knighton, W. B., Aiken, A. C., Gorkowski,
571 K. J., Dubey, M. K., Allan, J. D., and Thornton, J. A.: Contribution of Nitrated Phenols to Wood
572 Burning Brown Carbon Light Absorption in Detling, United Kingdom during Winter Time,
573 *Environ. Sci. Technol.*, 47, 6316-6324, <https://doi.org/10.1021/es400683v>, 2013.
- 574 Ni, H., Huang, R. J., Pieber, S. M., Corbin, J. C., and Dusek, U.: Brown Carbon in Primary and Aged
575 Coal Combustion Emission, *Environ. Sci. Technol.*, 55, 5701-5710,
576 <https://doi.org/10.1021/acs.est.0c08084>, 2021.
- 577 Olariu, R. I., Klotz, B. R., Barnes, I., Becker, K. H., and Mocanu, R.: FT-IR study of the ring-retaining
578 products from the reaction of OH radicals with phenol, o-, m-, and p-cresol, *Atmos. Environ.*,
579 36, 3685-3697, [http://doi.org/10.1016/S1352-2310\(02\)00202-9](http://doi.org/10.1016/S1352-2310(02)00202-9), 2002.
- 580 Ren, Y., Wang, G., Wei, J., Tao, J., Zhang, Z., and Li, H.: Contributions of primary emissions and
581 secondary formation to nitrated aromatic compounds in the mountain background region of
582 Southeast China, *Atmos. Chem. Phys.*, 23, 6835-6848, [http://doi.org/10.5194/acp-23-6835-](http://doi.org/10.5194/acp-23-6835-2023)
583 [2023](http://doi.org/10.5194/acp-23-6835-2023), 2023.
- 584 Ren, Y., Wei, J., Wang, G., Wu, Z., Ji, Y., and Li, H.: Evolution of aerosol chemistry in Beijing under
585 strong influence of anthropogenic pollutants: Composition, sources, and secondary formation
586 of fine particulate nitrated aromatic compounds, *Environ. Res.*, 204, 111982,
587 <https://doi.org/10.1016/j.envres.2021.111982>, 2022.
- 588 Ren, Y., Wei, J., Wu, Z., Ji, Y., Bi, F., Gao, R., Wang, X., Wang, G., and Li, H.: Chemical components
589 and source identification of PM_{2.5} in non-heating season in Beijing: The influences of biomass
590 burning and dust, *Atmos. Res.*, 105412, <https://doi.org/10.1016/j.atmosres.2020.105412>, 2021.
- 591 Ren, Y., Zhou, B., Tao, J., Cao, J., Zhang, Z., Wu, C., Wang, J., Li, J., Zhang, L., Han, Y., Liu, L., Cao,
592 C., and Wang, G.: Composition and size distribution of airborne particulate PAHs and
593 oxygenated PAHs in two Chinese megacities, *Atmos. Res.*, 183, 322-330,
594 <https://doi.org/10.1016/j.atmosres.2020.105412>, 2017.
- 595 Renhe, Z., Qiang, L. I., and Ruonan, Z.: Meteorological conditions for the persistent severe fog and haze
596 event over eastern China in January 2013, *Science China-earth Sciences*, 57, 26-35,
597 <http://doi.org/10.1007/s11430-013-4774-3>, 2014.
- 598 Sato, K., Hatakeyama, S., and Imamura, T.: Secondary Organic Aerosol Formation during the
599 Photooxidation of Toluene: NO_x Dependence of Chemical Composition, *J. Phys. Chem. A*, 111,
600 <http://doi.org/10.1021/jp071419f>, 2007.
- 601 Song, J., Li, M., and Zou, C.: Molecular Characterization of Nitrogen-Containing Compounds in Humic-
602 like Substances Emitted from Biomass Burning and Coal Combustion, *Environ. Sci. Technol.*,
603 56, 119-130, <https://doi.org/10.1021/acs.est.1c04451>, 2022.



- 604 Song, J., Zhu, M., Wei, S., Peng, P. A., and Ren, M.: Abundance and 14C-based source assessment of
605 carbonaceous materials in PM_{2.5} aerosols in Guangzhou, South China, *Atmos. Pollut. Res.*, 10,
606 313-320, <https://doi.org/10.1016/j.apr.2018.09.003>, 2018.
- 607 Sun, Y., Du, W., Fu, P., Wang, Q., Li, J., Ge, X., Zhang, Q., Zhu, C., Ren, L., and Xu, W.: Primary and
608 secondary aerosols in Beijing in winter: sources, variations and processes, *Atmos. Chem. Phys.*,
609 16, 8309-8329, <http://doi.org/10.5194/acp-16-8309-2016>, 2016.
- 610 Tan, J., Xiang, P., Zhou, X., Duan, J., Ma, Y., He, K., Cheng, Y., Yu, J., and Querol, X.: Chemical
611 characterization of humic-like substances (HULIS) in PM_{2.5} in Lanzhou, China, *Sci. Total
612 Environ.*, 573, 1481-1490, <http://dx.doi.org/10.1016/j.scitotenv.2016.08.025>, 2016.
- 613 Tan, T., Hu, M., Li, M., Guo, Q., Wu, Y., Fang, X., Gu, F., Wang, Y., and Wu, Z.: New insight into PM_{2.5}
614 pollution patterns in Beijing based on one-year measurement of chemical compositions, *Sci.
615 Total. Environ.*, 621, 734-743, <https://doi.org/10.1016/j.scitotenv.2017.11.208>, 2018.
- 616 Teich, M., Pinxteren, D. V., Kecorius, S., Wang, Z., Herrmann, H. J. E. S., and Technology: First
617 Quantification of Imidazoles in Ambient Aerosol Particles: Potential Photosensitizers, Brown
618 Carbon Constituents, and Hazardous Components, 50, 1166-1173,
619 <http://doi.org/10.1021/acs.est.5b05474> 2016.
- 620 Teich, M., Van Pinxteren, D., Wang, M., Kecorius, S., Wang, Z., Müller, T., Mocnik, G., and Herrmann,
621 H.: Contributions of nitrated aromatic compounds to the light absorption of water-soluble and
622 particulate brown carbon in different atmospheric environments in Germany and China, *Atmos.
623 Chem. Phys.*, 17, 1653-1672, <https://doi.org/10.5194/acp-17-1653-2017>, 2017.
- 624 Wang, G., Kawamura, K., Xie, M., Hu, S., Gao, S., Cao, J., An, Z., and Wang, Z.: Size-distributions of
625 n-alkanes, PAHs and hopanes and their sources in the urban, mountain and marine atmospheres
626 over East Asia, *Atmos. Chem. Phys.*, 9, 8869-8882, <http://doi.org/10.5194/acp-9-8771-2009>,
627 2009.
- 628 Wang, G., Zhang, R., Gomez, M. E., Yang, L., Levy, Z. M., Hu, M., Lin, Y., Peng, J., Guo, S., and Meng,
629 J.: Persistent sulfate formation from London Fog to Chinese haze, *Proc Natl Acad Sci U S A*,
630 113, 13630-13635, <https://doi.org/10.1073/pnas.1616540113>, 2016.
- 631 Wang, H., Gao, Y., Wang, S., Wu, X., Liu, Y., Li, X., Dandan, Huang, Lou, S., Wu, Z., Guo, S., Jing, S.,
632 Li, Y., Huang, C., Tyndall, G. S., Orlando, J. J., and Zhang, X.: Atmospheric Processing of
633 Nitrophenols and Nitrocresols From Biomass Burning Emissions, *J. Geophys. Res.-Atmos.*, 125,
634 <http://doi.org/10.1029/2020JD033401>, 2020a.
- 635 Wang, J., Wang, G., Gao, J., Wang, H., Ren, Y., Li, J., Zhou, B., Wu, C., Zhang, L., Wang, S., and Chai,
636 F.: Concentrations and stable carbon isotope compositions of oxalic acid and related SOA in
637 Beijing before, during, and after the 2014 APEC, *Atmos. Chem. Phys.*, 17, 981-992,
638 <http://doi.org/doi:10.5194/acp-17-981-2017>, 2017.
- 639 Wang, L., Wang, X., Gu, R., Hao, W., and Wang, W.: Observations of fine particulate nitrated phenols in
640 four sites in northern China: concentrations, source apportionment, and secondary formation,
641 *Atmos. Chem. Phys.*, 1-24, <https://doi.org/10.5194/acp-18-4349-2018>, 2018.
- 642 Wang, Y., Hu, M., Li, X., and Xu, N.: Chemical Composition, Sources and Formation Mechanisms of
643 Particulate Brown Carbon in the Atmosphere (in Chinese), *Progress in Chemistry*, 32, 627-645,
644 <http://doi.org/10.7536/PC190917>, 2020b.
- 645 Wang, Y., Hu, M., Wang, Y., Zheng, J., and Yu, J. Z.: The formation of nitro-aromatic compounds under
646 high NO_x and anthropogenic VOC conditions in urban Beijing, China, *Atmos. Chem. Phys.*, 19,



- 647 7649-7665, <https://doi.org/10.5194/acp-19-7649-2019>, 2019.
- 648 Wang, Y., Mehra, A., Krechmer, J. E., Yang, G., and Wang, L.: Oxygenated products formed from OH-
649 initiated reactions of trimethylbenzene: Autoxidation and accretion, *Atmos. Chem. Phys.*, 20,
650 9563-9579, <https://doi.org/10.5194/acp-20-9563-2020>, 2020c.
- 651 Wu, C., Wang, G., Li, J., Li, J., Cao, C., Ge, S., Xie, Y., Chen, J., Li, X., Xue, G., Wang, X., Zhao, Z.,
652 and Cao, F.: The characteristics of atmospheric brown carbon in Xi'an, inland China: sources,
653 size distributions and optical properties, *Atmos. Chem. Phys.*, 20, 2017-2030,
654 <https://doi.org/10.5194/acp-20-2017-2020>, 2020.
- 655 Xu, L., Duan, F., He, K., Ma, Y., Zhu, L., Zheng, Y., Huang, T., Kimoto, T., Ma, T., and Li, H.:
656 Characteristics of the secondary water-soluble ions in a typical autumn haze in Beijing, *Environ.*
657 *Pollut.*, 227, 296-305, <http://dx.doi.org/10.1016/j.envpol.2017.04.076>, 2017.
- 658 Yan, J., Wang, X., Gong, P., Wang, C., and Cong, Z.: Review of brown carbon aerosols: Recent progress
659 and perspectives, *Sci. Total. Environ.*, 634, 1475-1485,
660 <https://doi.org/10.1016/j.scitotenv.2018.04.083>, 2018.
- 661 Yi Chen, Penggang Zheng, Zhe Wang, Wei Pu, Yan Tan, Chuan Yu, Men Xia, Weihao Wang, Jia Guo,
662 Dandan Huang, Chao Yan, Wei Nie, Zhenhao Ling, Qi Chen, Shuncheng Lee, and Wang, T.:
663 Secondary Formation and Impacts of Gaseous Nitro-Phenolic Compounds in the Continental
664 Outflow Observed at a Background Site in South China, *Environ. Sci. Technol.*, 56, 6933-6943,
665 <https://doi.org/10.1021/acs.est.1c04596>, 2022.
- 666 Yuan, B., Liggio, J., Wentzell, J., Li, S. M., and Stark, H.: Secondary formation of nitrated phenols:
667 insights from observations during the Uintah Basin Winter Ozone Study (UBWOS) 2014,
668 *Atmos. Chem. Phys.*, 16, <http://doi.org/10.5194/acp-16-2139-2016>, 2016.
- 669 Zhang, Q., Shen, Z., Zhang, L., Zeng, Y., and Cao, J. J.: Investigation of Primary and Secondary
670 Particulate Brown Carbon in Two Chinese Cities of Xi'an and Hong Kong in Wintertime,
671 *Environ. Sci. Technol.*, 54, 3803-3813, <http://doi.org/10.1021/acs.est.9b05332>, 2020.
- 672 Zhang, R., Sun, X., Huang, Y., Shi, A., Yan, J., Nie, T., Yan, X., and Li, X.: Secondary inorganic aerosols
673 formation during haze episodes at an urban site in Beijing, China, *Atmos. Environ.*, 177, 275-
674 282, <https://doi.org/10.1016/j.atmosenv.2017.12.031>, 2018.
- 675 Zhang, W., Wang, W., Li, J., Ma, S., and Ge, M.: Light absorption properties and potential sources of
676 brown carbon in Fenwei Plain during winter 2018–2019, *JEnvS*, 102, 53-63,
677 <https://doi.org/10.1016/j.jes.2020.09.007>, 2021.
- 678 Zhao, M., Qiao, T., Li, Y., Tang, X., Xiu, G., and Yu, J.: Temporal variations and source apportionment
679 of Hulis-C in PM_{2.5} in urban Shanghai, *Sci. Total. Environ.*, 571, 18-26,
680 <http://doi.org/10.1016/j.scitotenv.2016.07.127>, 2016.
- 681 Zhu, C. S., Qu, Y., Zhou, Y., Huang, H., and Cao, J. J.: High light absorption and radiative forcing
682 contributions of primary brown carbon and black carbon to urban aerosol, *Gondwana Res.*, 90,
683 159-164, <https://doi.org/10.1016/j.gr.2020.10.016>, 2021.
- 684